Electrochemical Impedance Spectroscopy
of Alkaline Methanol Oxidation

Tanja Clees, Igor Nikitin, Lialia Nikitina,
Daniela Steffes-lai and Sabine Pott
Fraunhofer Institute for Algorithms and Scientific Computing
Sankt Augustin, Germany
Email: {Tanja.Clees|Igor.Nikitin
|Lialia.Nikitina|Daniela.Steffes-lai
|Sabine.Pott}@scai.fraunhofer.de

Ulrike Krewer and Theresa Windorfer
Institute of Energy and Process Systems Engineering
Technische Universität Braunschweig, Germany
Email: {u.krewer|t.windorfer}
@tu-braunschweig.de

Abstract—**Direct alkaline methanol fuel cell is a perspective technology for economic energy sources. The development of this technology requires advanced methods for the analysis of underlying chemical reactions. Electrochemical impedance spectroscopy is a popular method for analysis of dynamical processes in cells by a direct measurement of linear response function of the system to harmonic perturbations. In this paper, we propose a parameter identification procedure for electrochemical impedance spectroscopy of alkaline methanol oxidation. The procedure is based on decomposition of the linear response function in terms of poles and zeros and cross-fit of the obtained decomposition to the kinetic model using the methods of non-linear programming. The necessary conditions of the applicability of the proposed procedure have been derived and the stability of the method has been confirmed by the numerical experiments.**

Keywords–Modeling of complex systems; Non-linear optimization; Parameter identification; Applications; Electrochemistry.

I. INTRODUCTION

Methanol-powered fuel cells combine very high energetic density of methanol with the highly efficient energy converter concept of the fuel cell. Therefore, they are very attractive for portable and mobile power supplies. A widespread type of methanol fuel cells is based on acid medium, where the layers with a noble metal catalyst are used for accelerating the electrochemical oxidation of methanol. Since only platinum or platinum-ruthenium catalyst is sufficiently stable and active in an acid medium, the resulting material costs are very high, which makes these fuel cell systems less competitive. The costs can be reduced by the use of alkaline media, where the stability and activity of base metals, such as nickel, may approach that of platinum.

Electrochemical Impedance Spectroscopy (EIS) is a method for experimental analysis of dynamical electrochemical processes, based on a measurement of response of the system to harmonic oscillations of small amplitude over a wide frequency range [1–4]. The measured linear response function carries the information about kinetics of the electrochemical processes and allows to reconstruct the related reaction constants. Similar methods use signals of high amplitude to trigger non-linear effects, one can also use signals of different profiles, e.g., triangular signals of high amplitude are used in Cyclic Voltammetry (CV, [5], [6]), harmonic signals of high amplitude – in analysis of Total Harmonic Distortion (THD, [7]), etc.

Interpretation of the response is aided usually by model-based analysis. This commonly involves fitting of experimental data by parametric models using a kind of Non-linear Least Squares Fit (NLSF, [8], [9]). The problem becomes more difficult when complex processes are investigated, comprising many reagents and multiple chains of reactions. The reason is that the underlying kinetic models produce highly non-linear systems of equations of increasing size, impairing stability of the fit.

On the other hand, there are well established methods in electrotechnics, based on system identification in terms of poles and zeros of its transfer function. These methods are commonly used, e.g., in analysis of stability of power networks and electronic devices [10–12].

In this paper, we use a synergy of both approaches. At first, we perform a general system identification in terms of poles and zeros, with a possible cancellation of unstable elements. After that, the observed spectra are well described by a small number of parameters, for which a cross-fit to a kinetic model is performed. As a result, we reduce the dimension of the problem and improve stability of the fit.

The purpose of our work is to verify the stability of this procedure on the example of methanol oxidation in alkaline medium. Our motivation is triggered by the necessity of new design of the fuel cells allowing to reduce the costs of energetic resources. The goal is to develop a stable procedure for the determination of electrochemical kinetics in such systems. Synthetic data are used for the analysis, allowing to compare directly the specified and the reconstructed values of model parameters. This way, the precision of the reconstruction can be controlled.

In Section II, we describe a general problem setting in EIS analysis and the proposed parameter identification procedure. Section III is devoted to the details of kinetic model of methanol oxidation in alkaline medium. In Section IV, numerical experiments are presented and the obtained results are discussed.

II. ELECTROCHEMICAL IMPEDANCE SPECTROSCOPY

Electrochemical processes have kinetics described by a system of differential equations:

$$d\theta_i/dt = F_i(\theta, \eta), \ i = 1 \ldots n - 1, \quad (1)$$
$$d\eta/dt = F_n(\theta, \eta) + I_{cell}/C_{dl},$$

where θ_i are surface coverages of the electrode by adsorbed reagents, η is electrode potential, I_{cell} is cell current, C_{dl} is cell

capacitance. Details of (electro)chemical reactions are encoded in functions $F_{1...n}$. These functions are generally polynomial w.r.t. θ_i, while η-dependence has exponential form, defined by Tafel equation: $\exp(\pm \alpha F/(RT) \cdot \eta)$. Here, α is charge transfer coefficient, F is Faraday constant, R is universal gas constant, T is absolute temperature. The measurable quantities in these equations are η and I_{cell}, while the detailed dynamics of variables θ_i is not directly measurable. Particular reactions define the form of the polynomials, while the coefficients are defined by reaction constants, which are generally unknown. Parameter identification, EIS method in particular, has the purpose of reconstructing the reaction constants from the measured data.

Let us consider a stationary point of the system (1):

$$0 = F_i(\theta^*, \eta^*), \ i = 1 \ ... \ n-1, \qquad (2)$$
$$0 = F_n(\theta^*, \eta^*) + I_{cell}^*/C_{dl},$$

and linearize the system in this point:

$$dv/dt = Jv + b, \ J_{ij} = \partial F_i/\partial x_j. \qquad (3)$$

Here, J is $n \times n$ Jacobi matrix, evaluated in stationary point, $x = (\theta_1, ..., \theta_{n-1}, \eta)^T$ is n-dimensional vector of variables, $v = \delta x$, $b = (0, ..., 0, \delta I_{cell}/C_{dl})^T$ are variations of vectors. Equations (3) define the evolution of the system near the stationary point, when the current (or potential) is varied according to a given profile. In EIS method, the harmonic profiles are taken, in complex denotation: $\delta \eta = \eta_0 \exp(i\omega t)$, $\delta I_{cell} = I_0 \exp(i\omega t)$, while their ratio gives a transfer function, or complex resistance, impedance $Z = \eta_0/I_0$. Harmonic substitution $v = v_0 \exp(i\omega t)$, $b = b_0 \exp(i\omega t)$ transforms (3) to

$$(i\omega - J)v_0 = b_0 \qquad (4)$$

and we obtain as a result:

$$C_{dl}Z(\omega) = ((i\omega - J)^{-1})_{nn}. \qquad (5)$$

This expression can be written in a rational form

$$C_{dl}Z(\omega) = Q_{n-1}(i\omega)/Q_n(i\omega), \qquad (6)$$

i.e., as a ratio of two polynomials of $(n-1)$-th and n-th degree, respectively. Here, the denominator represents the determinant of the matrix $(i\omega - J)$ and nominator – its (n, n)-minor. For the rational functions, the following equivalent representations are often used:

$$C_{dl}Z(\omega) = \prod_{j=1}^{n-1}(i\omega - q_j)/\prod_{j=1}^{n}(i\omega - p_j), \qquad (7)$$

where p_j are poles and q_j are zeros of Z, or

$$C_{dl}Z(\omega) = \sum_{j=1}^{n} r_j/(i\omega - p_j), \qquad (8)$$

where r_j are residues at the poles p_j. Equivalently, p_j are eigenvalues of Jacobi matrix J and q_j are eigenvalues of its left-upper $(n-1) \times (n-1)$ submatrix.

The curve $Z(\omega)$ on a complex plane is known as Nyquist plot, see Figure 1 left. Z is a complex resistance (impedance, in Ohm), ω is cyclic frequency (in rad/s). The green curve corresponds to experimentally relevant positive values of ω.

The red curve corresponds to negative ω, artificially introduced to represent complete rational curves, closed by complex conjugation.

The plot on Figure 1 left represents a typical measurement result in the EIS method. To obtain decomposition of impedance in form (7) or (8), one can use rational fitting techniques. There is a variety of methods and software packages available for this purpose [13–15]. The forms (7),(8) can also be directly fitted to experimental data with general purpose optimizing routines [16–19]. These procedures are known to be extremely robust. They encode the whole set of measured curves in a small number of poles and zeros, giving a compact equivalent representation of the experimental data for further fits.

The advantage of poles-zeros representation is not only improvement of stability of fitting procedures, but also determination of important characteristics of electrochemical kinetics. In particular, the poles are eigenvalues of Jacobi matrix which determine such processes as relaxation of the system to the stationary state, delay and hysteresis effect in high-amplitude dynamic scans of the cell, etc.

Figure 1 right shows a typical pattern of poles and zeros displayed on a complex plane. In the considered case all eigenvalues are real, negative and strongly hierarchical, here shown in logarithmic scale. Indeed, in view of the stability of the system, the poles should be located at Re < 0, they can be real-valued (corresponding to exponential decay of $\exp(pt)$) or form complex conjugated pairs (corresponding to decaying oscillations). Closely located poles and zeros can be canceled from nominator and denominator of (7). Generally this will only influence small local features near the canceled poles and zeros, producing the effects under the limit of experimental precision, while the rest of the function will not be changed [10]. The cancellation can be useful, since it reduces the degrees of polynomials and a number of constraints used for cross-fit.

Cross-fit matches the reaction constants to the obtained pattern of poles and zeros. It can be formulated as a generic problem of Non-Linear Programming (NLP, [20]):

$$\text{find } \min_x f(x), \text{ such that } g(x) = 0 \text{ and } h(x) \geq 0, \quad (9)$$

i.e., minimization of an objective function in a domain, specified by equality and inequality constraints. In our application, the optimization variables x combine the reaction constants k_r entering in (1) and position of stationary point θ^* in (2). The functions g collect the equations for stationary point (2), the definition of Jacobi matrix in (3) and the definition of poles and zeros:

$$Q_{n-1}(q_j) = 0, \ Q_n(p_j) = 0. \qquad (10)$$

In these equations, Q are recorded in terms of the minors, while q, p are set to the values found from experimental data. The inequalities provide non-negativity of reaction constants and surface coverage:

$$k_r \geq 0, \ \theta_i^* \geq 0, \ \theta_0^* = 1 - \sum \theta_i^* \geq 0. \qquad (11)$$

In the case if the number of equality constraints becomes greater than the number of optimization variables (overdetermined problem), a part of the constraints should be moved to
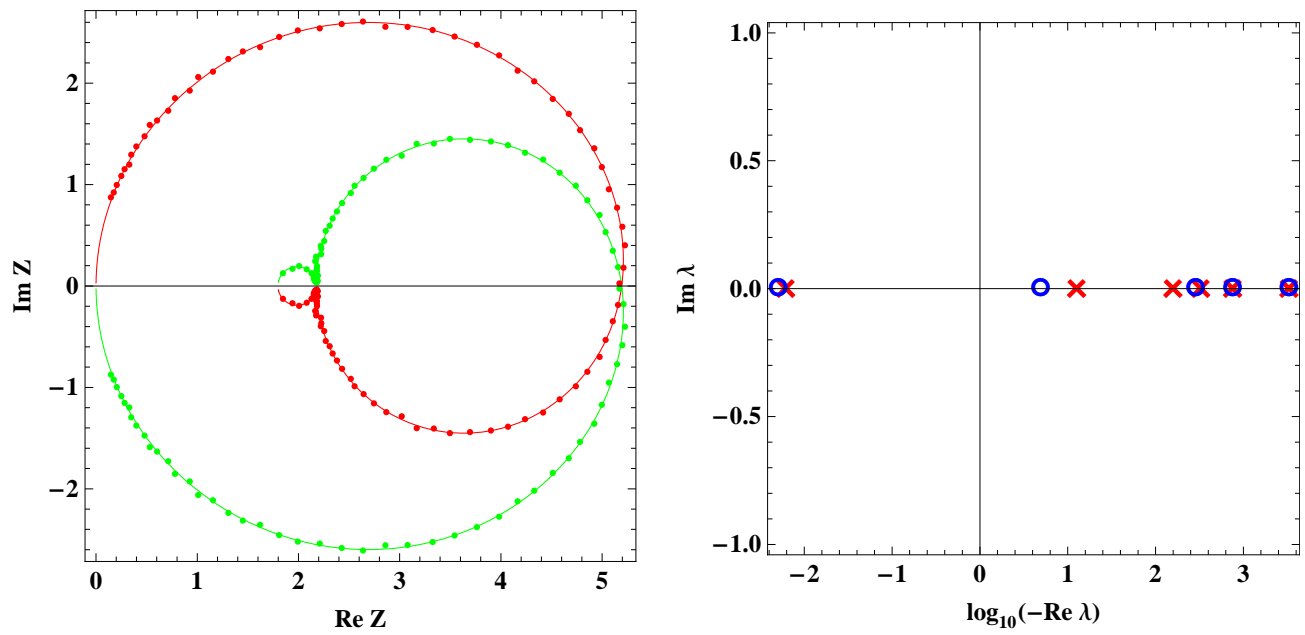
Figure 1. On the left: Nyquist plot $\text{Re}(Z(\omega)), \text{Im}(Z(\omega))$ for synthetic data. On the right: position of poles (red crosses) and zeros (blue circles) on the complex plane, formed by eigenvalues of linearized problem. See details in the text.
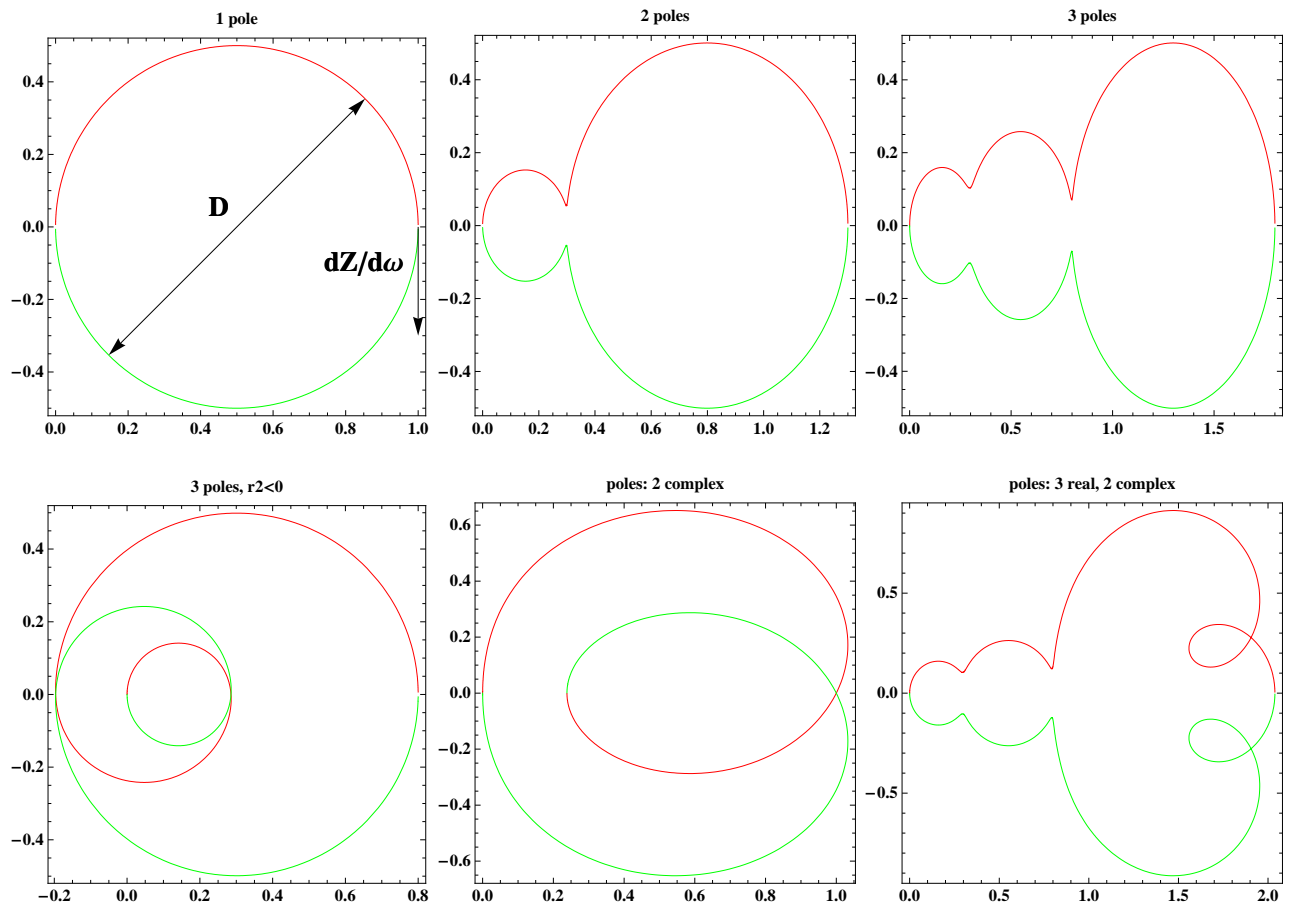
Figure 2. Nyquist plots for different types of the rational curves. The upper sequence shows the case of hierarchically separated real poles with positive residues. The bottom sequence shows the influence of the sign of the residue and the effects of complex poles.

the objective function, e.g.:

$$f(x): \chi^2 = \sum_j |Q_{n-1}(q_j)|^2 + \sum_j |Q_n(p_j)|^2. \quad (12)$$

There is a number of general purpose optimizing routines [16–19], suitable for the solution of so formulated problem.

We prefer to use algorithm *NMinimize* from Mathematica [16], since it comprises strategies for finding a global optimum and can be easily combined both with derivative-based and derivative-free optimization methods. Mathematica also possesses powerful capabilities for formulating the equations, computing partial derivatives in analytical form and provides a convenient interface for the modeling of complex dynamical systems. Typically, in the considered electrochemical problem *NMinimize* converges to the optimum in 5000 iterations, taking 35 minutes on 3GHz CPU.

The description in terms of poles and zeros (or residues) specifies a rich family of rational curves. Some typical representatives are shown in Figure 2. A single real pole defines a semi-circular arc. It closes the complete circle through the domain of negative frequencies, formally representing a complex conjugation of the transfer function. The diameter of the circle D and the derivative $dZ/d\omega$ are defined by values of the pole and the residue: $D = |r/p|$, $|dZ/d\omega| = |r|/p^2$, $C_{dl} = 1$. Several poles give a combination of several arcs. If the poles are hierarchically separated: $|p_1| \ll |p_2| \ll |p_3|...$, there will be several clearly visible arcs, shown on upper sequence on Figure 2. The bottom sequence on Figure 2 shows the influence of the sign of the residue as well as the effects of complex poles, creating typical windings on the curves.

Analyzing the influence of noise in Nyquist data to the determination of poles and zeros, take a variation of (7):

$$\delta Z(\omega)/Z(\omega) = -\sum \delta q_j/(i\omega - q_j) \quad (13)$$
$$+ \sum \delta p_j/(i\omega - p_j).$$

In the case when the poles and/or zeros start to collide, i.e., there are nearly coincident complex numbers in the set of $\{q_j, p_j\}$, one can form unstable combinations, e.g.,

$$(\delta p_1 + \delta p_2)/(i\omega - p_{1,2}) \text{ at } p_1 \approx p_2. \quad (14)$$

In this way, one can select an arbitrary large but compensating variation of the poles without significant variation of the Nyquist plot. As a result, the reconstruction of such poles and zeros becomes unstable. This situation includes the case when a pole-zero pair wanders randomly on the complex plane without actual influence to the observable data. It also includes the cases when pole-pole or zero-zero collisions happen, e.g., collision of two real poles leading to their transformation to a complex conjugated pair. All such cases are highly singular and sensitive to the influence of noise in data.

In the case when poles and zeros are well separated from each other, the functions $(i\omega - q_j)^{-1}$, $(i\omega - p_j)^{-1}$ form linearly independent set. In this case vanishing variations of $Z(\omega)$ correspond to vanishing variations of poles and zeros, so that the reconstruction becomes more stable.

In the case if poles and zeros are hierarchically separated, i.e., well separated in logarithmic scale, the stability of reconstruction is drastically increased. The reason is that every pole and zero contributes to a wide range of frequencies, containing a lot of the measurement points ($N_{pt} \gg 1$). This leads to statistical improvement of precision by a factor of $\sqrt{N_{pt}}$, for

the reconstructed poles and zeros in comparison to the noise in Nyquist data.

III. ALKALINE METHANOL OXIDATION

For the description of alkaline methanol oxidation, we will use the following model, based on the analysis of experimental data from [6].

Reactions:

$$r_1: \quad OH^- + Pt \rightleftharpoons OH_{ad} + e^-$$
$$r_2: \quad CH_3OH + Pt \rightleftharpoons CH_3OH_{ad}$$
$$r_3: \quad CH_3OH_{ad} + 3\,OH_{ad} \rightleftharpoons CHO_{ad} + 3\,H_2O$$
$$r_4: \quad CHO_{ad} + OH_{ad} \longrightarrow CO_{ad} + H_2O$$
$$r_5: \quad CO_{ad} + 2\,OH_{ad} \longrightarrow CO_2 + H_2O + 2\,Pt$$
$$r_7: \quad CHO_{ad} + 2\,OH_{ad} \longrightarrow COOH_{ad} + H_2O + Pt$$
$$r_8: \quad COOH_{ad} + e^- \rightleftharpoons HCOO^- + Pt$$
$$r_9: \quad CO_{ad} + OH_{ad} \longrightarrow COOH_{ad} + Pt$$
$$r_{10}: \quad COOH_{ad} + OH_{ad} \longrightarrow CO_2 + H_2O + 2\,Pt$$
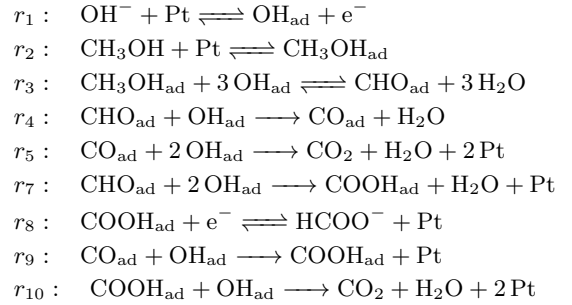
The corresponding formal reaction kinetics and the charge balance yield the following set of equations:

$$F_1 = (r_1 - 3r_3 - r_4 - 2r_5 - 2r_7 - r_9 - r_{10})/C_{act},$$
$$F_2 = (r_2 - r_3)/C_{act},$$
$$F_3 = (r_3 - r_4 - r_7)/C_{act},$$
$$F_4 = (r_4 - r_5 - r_9)/C_{act}, \quad (15)$$
$$F_5 = (r_7 - r_8 + r_9 - r_{10})/C_{act},$$
$$F_6 = (-r_1 + r_8) \cdot FA/C_{dl},$$

where

$$r_1 = k_1 c_1 \theta_0 - k_{-1}\theta_1, \quad r_2 = k_2 c_2 \theta_0 - k_{-2}\theta_2,$$
$$r_3 = k_3 \theta_2 \theta_1^3 - k_{-3}\theta_3 c_3^3, \quad r_4 = k_4 \theta_3 \theta_1,$$
$$r_5 = k_5 \theta_4 \theta_1^2, \quad r_7 = k_7 \theta_3 \theta_1^2, \quad r_8 = k_8 \theta_5, \quad (16)$$
$$r_9 = k_9 \theta_4 \theta_1, \quad r_{10} = k_{10}\theta_5 \theta_1, \quad \theta_0 = 1 - \sum_1^5 \theta_i,$$
$$k_1 = k_1^0 \exp(\alpha\beta\eta), \quad k_{-1} = k_{-1}^0 \exp(-(1-\alpha)\beta\eta),$$
$$k_8 = k_8^0 \exp(-(1-\alpha)\beta\eta), \quad \beta = F/(RT).$$

The parameters in the equations are described in Tables I-III. Additional constants, introduced here are: c_i – mole fractions of the reagents, C_{act} – surface concentration of catalyst, A – geometric electrode area.

TABLE I. NUMERATION OF VARIABLES AND CONSTANTS.

θ_1	OH_{ad}		
θ_2	CH_3OH_{ad}	c_1	OH^-
θ_3	CHO_{ad}	c_2	CH_3OH
θ_4	CO_{ad}	c_3	H_2O
θ_5	$COOH_{ad}$		

For generation of synthetic data for numerical experiments, we specify reaction constants as given in Table III. Then we find a stationary point by solving (2), Jacobi matrix by (3), impedance function by (5) and its poles and zeros by (7). The function is displayed on Figure 1 left and its poles and zeros

TABLE II. MODEL CONSTANTS.

Constant, units	Value
F, C/mol	$9.649 \cdot 10^4$
R, J/(K mol)	8.314
T, K	303.35
η^*, V	-0.3
A, m^2	$1.96 \cdot 10^{-5}$
C_{dl}, F	10^{-3}
C_{act}, mol/m^2	$1.424 \cdot 10^{-4}$
α	0.5

TABLE III. REACTION CONSTANTS.

Constant [mol/(m$^2 s$)]	Specified	Reconstructed
k_1^0	$1.056 \cdot 10^2$	$1.056 \cdot 10^2$
k_{-1}^0	10^{-5}	$0.966 \cdot 10^{-5}$
k_2	$5.672 \cdot 10^{-1}$	$5.665 \cdot 10^{-1}$
k_{-2}	10^{-5}	$0.966 \cdot 10^{-5}$
k_3	$3.629 \cdot 10^3$	$3.629 \cdot 10^3$
k_{-3}	10^{-5}	$3.554 \cdot 10^{-5}$
k_4	10^{-5}	$1.008 \cdot 10^{-5}$
k_5	$3.697 \cdot 10^{-4}$	$3.921 \cdot 10^{-4}$
k_7	$6.192 \cdot 10^1$	$6.192 \cdot 10^1$
k_8^0	10^{-5}	$1.037 \cdot 10^{-5}$
k_9	10^{-5}	$0.984 \cdot 10^{-5}$
k_{10}	$7.879 \cdot 10^{-1}$	$7.879 \cdot 10^{-1}$

on Figure 1 right. Then we add a noise on the level of 3%, as shown by points on Figure 1 left, to simulate typical scatter in experimental data.

IV. PARAMETER IDENTIFICATION

Solving the inverse problem, we take the noisy points on Figure 1 as input data and fit them by the rational function (8). The obtained poles and residues are used to find zeros in (7). Closely located poles and zeros are canceled. The remaining poles and zeros are used to reconstruct reaction constants by cross-fit procedure (9)-(12). Estimating the number of variables and equations in this procedure, we see that stable reconstruction is possible if the number of experiments N_{exp}, the number of obtained poles and zeros per experiment $N_{p,z}$ and the number of the reaction constants N_k satisfy the condition $N_{exp}(N_p + N_z + 1) \geq N_k$. In our case 2 experiments are sufficient for stable reconstruction. In the experiments we set different methanol concentrations 0.1mol/l and 0.075mol/l, while alkaline concentration was set to 1mol/l and 0.7mol/l respectively.

The result is shown in the right column of Table III. The reconstructed reaction constants are close to the specified values, 6 constants are reconstructed with the precision <1% and 5 constants with the precision in the range 1%-5%. One constant, k_{-3}, is increased by a factor of 3 after the reconstruction. The contribution of this constant in the reaction r_3, with account of all θ-factors, is much smaller than the neighbour contribution of k_3. This is the reason why the constant k_{-3} is reconstructed less precisely than the others.

In summary, our numerical experiment demonstrates that the reconstruction procedure generally does not amplify the noise in transition from input data to model parameters, except of the constants giving a negligible contribution to the reactions. Therefore, the proposed procedure is robust enough for the usage in practical applications of parameter identification in electrochemical impedance spectroscopy.

There are some possible modifications of the procedure. There are special cases, when the stationary point becomes inaccessible for experimental measurements, e.g., due to the effects of electrode poisoning with intermediates or byproducts of reactions, which can happen before the stationary point is reached. The described methodology is still applicable in this non-stationary situation, if the linearization point θ^* performs only a little change during the recording of EIS diagram. In such case the stationary equations (2) should be removed from the system, while the condition on poles and zeros (10) will remain in force. The condition of stable reconstruction becomes $N_{exp}(N_p + N_z - n + 1) \geq N_k$. This condition can be satisfied at sufficient number of poles and zeros per experiment $N_p + N_z > n - 1$ and sufficiently large number of experiments.

Such quasistationary approximation can be used for estimation of parameters and obtaining a starting point for more sophisticated methods. Currently, we are performing various measurements of alkaline-methanol oxidation in our laboratory in Braunschweig. They include not only EIS experiments, but also CV, THD, etc. Their analysis is similar, but due to the non-linear effects involved they require numerical integration and is, therefore, more complex. In particular, the search for the optimum requires extensive Monte Carlo runs with a typical complexity 120000 points per 6 hours on 3GHz CPU.

V. CONCLUSION

We have proposed a parameter identification procedure for electrochemical impedance spectroscopy of alkaline methanol oxidation process. The procedure is based on decomposition of the measured linear response function in terms of poles and zeros, elimination of unstable elements and the cross-fit of the obtained decomposition to the kinetic model. The cross-fit is solved with the methods of non-linear programming. The number of experiments, necessary for stable reconstruction, is estimated. Numerical experiments are performed, demonstrating stability of the method.

With the developed method, two experiments with a typical Nyquist plot, shown on Figure 1, representing a problem with 12 parameters, 24 inequality constraints and containing 3% noise, have been analyzed. The kinetic is reconstructed in 5000 iterations, taking 35 min on 3GHz CPU. The precision of the reconstruction is <1% for 6 reaction constants, 1%-5% for 5 reaction constants. One constant has a negligible contribution in the reactions and escapes the identification.

REFERENCES

[1] U. Krewer, T. Vidakovic-Koch, L. Rihko-Struckmann, "Electrochemical oxidation of carbon-containing fuels and their dynamics in low-temperature fuel cells", ChemPhysChem, vol. 12, 2011, pp. 2518-2544.

[2]   U. Krewer, M. Christov, T. Vidakovic, K. Sundmacher, "Impedance spectroscopic analysis of the electrochemical methanol oxidation kinetics", Journal of Electroanalytical Chemistry, vol. 589, 2006, pp. 148-159.

[3]   F. Ciucci, "Revisiting parameter identification in electrochemical impedance spectroscopy: Weighted least squares and optimal experimental design", Electrochimica Acta, vol. 87, 2013, pp. 532-545.

[4]   Gamry Instruments, Basics of Electrochemical Impedance Spectroscopy, online tutorial, http://www.gamry.com/application-notes/EIS/basics-of-electrochemical-impedance-spectroscopy [accessed: 2017-04-24]

[5]   A. J. Bard and L. R. Faulkner, Electrochemical Methods: Fundamentals and Applications, Wiley 2000.

[6]   B. Beden, F. Kardigan, C. Lamy, J. M. Leger, "Oxidation of methanol on a platinum electrode in alkaline medium: effect of metal ad-atoms on the electrocatalytic activity", J. Electroanalytical Chem., vol. 142, 1982, pp. 171-190.

[7]   Q. Mao and U. Krewer, "Total harmonic distortion analysis of oxygen reduction reaction in proton exchange membrane fuel cells", Electrochimica Acta, vol. 103, 2013, pp. 188-198.

[8]   W. H. Press, S. A. Teukolsky, W. T. Vetterling, B. P. Flannery, Numerical Recipes in C, Cambridge University Press 1992, Chap. 15.

[9]   T. Strutz, Data Fitting and Uncertainty: A practical introduction to weighted least squares and beyond, Springer 2016.

[10]   M. I. Bryzgunov, A. D. Goncharov, V. B. Reva, D. N. Skorobogatov, "Determination of transfer function of regulated object by characteristics of closed system with feedback", Reports of Novosibirsk State University, vol. 3, 2008, pp. 104-113, in Russian.

[11]   B. Gustavsen and A. Semlyen, "Combined phase and modal domain calculation of transmission line transients based on vector fitting", IEEE Trans. Power Delivery, vol. 13, 1998, pp. 596-604.

[12]   B. Gustavsen, "Wide band modeling of power transformers", IEEE Trans. Power Delivery, vol. 19, 2004, pp. 414-422.

[13]   B. Gustavsen and A. Semlyen, "Rational approximation of frequency domain responses by vector fitting", IEEE Trans. Power Delivery, vol. 14, 1999, pp. 1052-1061.

[14]   R. Zeng and J. Sinsky, "Modified Rational Function Modeling Technique for High Speed Circuits", IEEE MTT-S Int. Microwave Symp. Dig., San Francisco, CA, June 11–16, 2006.

[15]   Rational Fitting Algorithm, MathWorks, https://de.mathworks.com/help/rf/ug/rationalfit.html [accessed: 2017-04-24]

[16]   NMinimize Algorithm, Mathematica, http://reference.wolfram.com/language/ref/NMinimize.html [accessed: 2017-04-24]

[17]   Interior Point OPTimizer, IPOPT, https://projects.coin-or.org/Ipopt [accessed: 2017-04-24]

[18]   Sparse Nonlinear OPTimizer, SNOPT, http://www.sbsi-sol-optimize.com/asp/sol_product_snopt.htm [accessed: 2017-04-24]

[19]   Modular In-core Nonlinear Optimization System, MINOS, http://www.sbsi-sol-optimize.com/asp/sol_product_minos.htm [accessed: 2017-04-24]

[20]   A. Wächter and L. T. Biegler, "On the implementation of an interior-point filter line-search algorithm for large-scale nonlinear programming", Mathematical Programming, vol. 106, 2006, pp. 25-57.